


Article

Saw Filters Vibrational Sensitivity Characterization

Massimiliano Rossi ^{1,†,‡} ¹ MBDA Italia S.p.A. Via Monte Flavio, 45 - 00131 - Roma - Italy; massimiliano.rossi@mbda.it

Abstract: A novel characterization method for discrete saw filters vibrational sensitivity is presented. The proposed approach allows the characterization of filters under vibrations and the extraction of a behavioural model. Filters are assumed to be transducers so that external induced vibrational energy is partially transformed in a undesired simultaneous amplitude and phase modulation of the input RF signal. When the filter is mechanically excited with vibrations, it introduces spurious amplitude and phase modulation to the input signal that can potentially affect the link quality.

Keywords: microwave filters; vibration sensitivity; acoustic noise

1. Introduction

Filtering stages are fundamental blocks in all communication systems from mobile terminals to complex aerospace and defence ones. When volumes and weights are limited and good electrical performance must be guaranteed, a plethora of new technologies seems available to the system designer. Surface Acoustic Wave (SAW) or Dielectric Resonator (DR) filters, for example, appear to be ideal candidates. A big concern arises when severe or very hard environmental conditions have to be taken into account, such environments are well known in the aerospace and defence fields [1]. Besides high temperature variations there is a big concern about the presence of mechanical vibrations even at acoustic frequencies with very high pressure levels. Undesired phenomena generated by vibrations are well known also in crystal oscillators [2] where some fundamental figure of merit are currently available. Vibrational energy can affect the electrical performance of filtering stages introducing spurious signal modulations that can degrade the RF link quality. In this paper it is proposed a novel characterisation method that can be used to model the vibration sensitivity of saw filters when subjected to vibrational energy.

2. General theory and characterization technique

Induced phase noise characterisation methods as well vibration sensitivity figure of merit for filters [3][4] are available, but from these it is not easy to directly infer behavioural models of discrete microwave filters. Usually, manufacturers perform vibration and shock tests according to international standards [5] [6] [7] in order to certify that the devices meet electrical performance *after* the trials [8], but sometimes evidence of correct operation of the device is required *during* the application of the solicitation. A filter subjected to vibrations can be reasonably treated as a transducer so that external induced vibrational energy is partially transformed in simultaneous amplitude and phase modulation of the input RF or IF signal. The signal bandwidth is supposed to be much wider than the vibration induced modulation bandwidth. The theory of operation can be understood by referring to the test-bed reported in Figure 1. Using a compact complex envelope notation [9], the RF source generates an in-band CW (Continuous Wave) signal:

$$i_i(t) = A_0 e^{j\varphi_0} \quad (1)$$

at node *A* of the circuit where it is splitted in two paths: *upper* and *lower*. The signal in the *upper* path

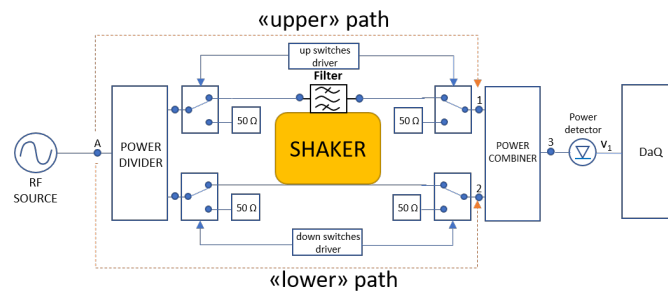


Figure 1. Characterisation set-up

flows through the filter where emerges modulated both in amplitude and phase due to the vibrational energy as:

$$i_o(t) = A_o m_F(t) e^{[j\phi_o + j\psi_F(t)]} \quad (2)$$

with $0 \leq m_F(t) \leq 1$. The signal in the *lower* path flows in a through-line and recombines with the signal coming from the *upper* path in an isolated RF combiner. The signals flow is regulated by two couples of SPDTs (Single Pole Double Throw) in order to provide high isolation level: the first couple controls the *upper* path; the second couple controls the *lower* path. Each couple of SPDT is driven by a dedicated driver. The signal from the output RF combiner is injected in a zero bias schottky detector whose output signal, being eventually conveniently amplified by a low noise stage, is acquired. A dedicated fixture is designed and fixed to the shaker to allow vibration tests to be performed. The filter, generally available in a SMT package (Surface Mount Technology), is soldered over a microstrip circuit with dedicated input and output connectors. A microstrip through line is located near the filter with its own input and output connectors. So, two input ports and two output ports are available on the test jig, each circuit is independent from the other but both shares the same vibrational energy. Following the scheme, it is possible to note that the jig, fixed to the shaker, is connected to the isolated RF power divider and combiner using phase invariant coaxial cables so that when the SPDTs are driven as in Figure 2, it is possible to identify an *upper* and *lower* path where the input signal is first splitted and

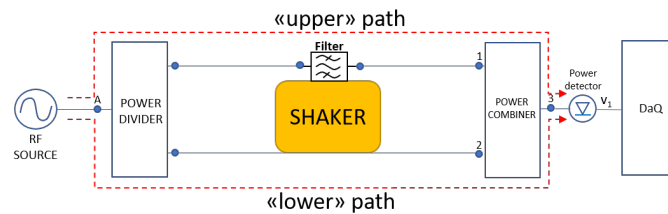


Figure 2. General characterisation set-up

then recombined. Using the superposition principle, the input signal to the power detector due to the *upper* path is:

$$S_{out1}(t) = A_o S_{3Au} m_F(t) e^{[j\psi_F(t) + j\phi_{3Au}]} \quad (3)$$

23 where:

- 24 1. $S_{3Au} e^{j\phi_{3Au}}$ is the transmittance from port A to port 3 through the *upper* path when there is no
- 25 vibration
- 26 2. $m_F(t) e^{j\psi_F(t)}$ is the instantaneous transmittance of the filter under vibrations and $\psi_F(t)$ is a real
- 27 valued function

while the input signal to the power detector due to the *lower* path is:

$$S_{out2}(t) = A_o S_{3Ad} m_d(t) e^{[j\psi_d(t) + j\phi_{3Ad}]} \quad (4)$$

28 where:

- 29 1. $S_{3Ad}e^{j\phi_{3Ad}}$ is the transmittance from port A to port 3 through the *lower* path when there is no
 30 vibration
 31 2. $m_d(t)e^{j\psi_d(t)}$ is the instantaneous transmittance of the microstrip line under vibration, being $\psi_d(t)$
 32 a real valued function

so, the *recombined output signal* arising from the RF combiner can be put in the form:

$$S_{out}(t) = A_o S_{3Ad} m_d(t) e^{[j\psi_d(t) + j\phi_{3Ad}]} + A_o S_{3Au} m_F(t) e^{[j\psi_F(t) + j\phi_{3Au}]} \quad (5)$$

this signal is injected in a zero bias schottky detector, whose output signal is of the form:

$$v_1(t) = k_d P_i(t) \quad (6)$$

where k_d is the detector's sensitivity and $P_i(t)$ the instantaneous power of the RF input signal. When the system is under vibration, the instantaneous output signal is:

$$v_1(t) = A_o^2 k_d (2S_{3Ad} S_{3Au} m_d(t) m_F(t) \cos(\psi_d(t) + \phi_{3Ad} - \psi_F(t) - \phi_{3Au}) + S_{3Ad}^2 m_d(t)^2 + S_{3Au}^2 m_F(t)^2) \quad (7)$$

while, when no vibrational energy is injected to the system:

$$v_{1_static} = A_o^2 k_d (2S_{3Ad} S_{3Au} \cos(\phi_{3Ad} - \phi_{3Au}) + S_{3Ad}^2 + S_{3Au}^2) \quad (8)$$

so, v_{1_static} , is time independent. If the filter's microphonicity is negligible, the output signal is constant. If the microstrip circuit, that's part of the *lower path*, can be assumed to be quite insensible to vibrations, it's possible to simplify the output signal as:

$$v_1(t) = A_o^2 k_d (2S_{3Ad} S_{3Au} m_F(t) \cos[\phi_{3Ad} - \psi_F(t) - \phi_{3Au}] + S_{3Ad}^2 + S_{3Au}^2 m_F(t)^2) \quad (9)$$

now, when the SPDT couple of the down path is driven in order to open the signal's flow, the test-bed is equivalent to Figure 3. The output signal, under vibration, is:

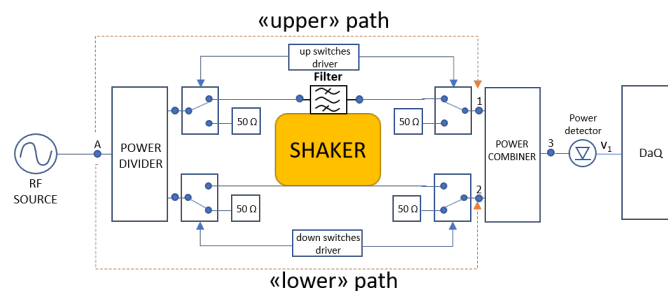


Figure 3. Characterisation set-up with *lower* path opened

$$v_{1_down_o_vibr}(t) = A_o^2 k_d S_{3Au}^2 m_F(t)^2 \quad (10)$$

while, in static conditions:

$$v_{1_down_open_static} = A_o^2 k_d S_{3Au}^2 \quad (11)$$

when the SPDT couple of the *upper* path is driven in order to open the signal's flow, the test-bed is equivalent to that reported in Figure 4. The output signal, under vibration and in static condition, is:

$$v_{1_up_o_vibr} = v_{1_up_o_static} = A_o^2 k_d S_{3Ad}^2 \quad (12)$$

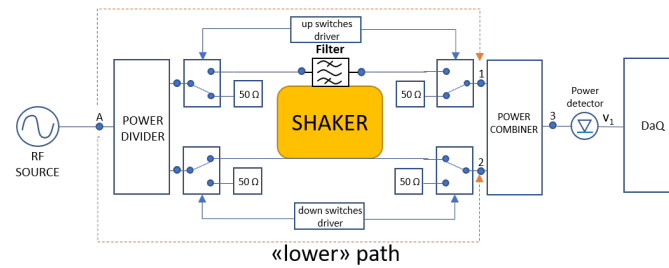


Figure 4. Characterisation set-up with upper path opened

so the filter amplitude modulation, if present, constitutes the signal:

$$v_{1_down_o_vibr}(t) = A_0^2 k_d S_{3Au}^2 m_F(t)^2 \quad (13)$$

If the DC component is prevalent, then the amplitude modulation is negligible and $m_F(t)^2 \cong 1$. Under these conditions the signals: $v_{1_down_o_vibr}(t)$, $v_{1_up_o_vibr}$, $v_{1_down_o_vibr}(t)$ are DC voltages and the phase induced modulation function $\psi_F(t)$ is recoverable from the output signal:

$$v_1(t) = 2A_0^2 k_d S_{3Au} S_{3Ad} \cos(\psi_F(t) + \phi_0) + A_0^2 k_d S_{3Ad}^2 + A_0^2 k_d S_{3Au}^2 \quad (14)$$

33 apart from a constant phase term $\phi_0 = \phi_{3Au} - \phi_{3Ad}$. The vibration induced phase modulation $\psi_F(t)$
 34 is transformed in a *amplitude modulation* of the low frequency signal $v_1(t)$, so a wise choice of the phase
 35 term ϕ_0 allows to maximize the signal's dynamic range. If the low signal phase difference between
 36 upper and lower paths $\phi_0 = (2n + 1)\frac{\pi}{2}$ with $n \in \mathbb{Z}$, than the slope of the cosine function in equation
 37 (14) is maximized. Changing the vibrational sine frequency, it's possible to extract the relative induced
 38 phase modulation and the characterization process can be fully automated.

39 2.1. System Simulation and Validation

40 The theoretical approach has been validated through RF system simulations using NI AWR VSS
 41 Visual System SimulatorTM [10] and MATLAB[®] [11]. The NI AWR VSS schematic is reported in Figure
 5 and includes, in a more detailed form, the characterisation set-up depicted in Figures 3 and 4. A

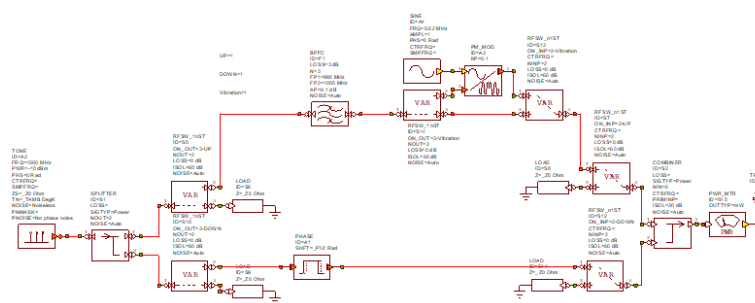


Figure 5. Characterisation set-up VSS system model

42 signal generator injects a -10 dBm CW tone at 1 GHz into a power divider where it is divided in two
 43 branches. The upper path contains an RF filter, in this case a 3 poles, 10 MHz bandwidth Bandpass
 44 Chebyshev type 1 filter with an insertion loss of 3 dB, followed by a *phase modulator that represents the*
 45 *induced phase modulation due the vibrational energy*. The vibration induced phase modulating signal is a
 46 20 KHZ unit amplitude sine wave injected in a phase modulator with a phase sensitivity coefficient
 47 $K_p = 0.1$. The presence or absence of vibrations and the path selection is performed by dedicated
 48 SPDTs whose insertion loss take into account the additional losses introduced by the cables also. The
 49

50 lower path contains the dedicated branch selection SPDTs, cable and a RF phase shifter. The signals
 51 arising from the upper and lower paths are injected in a RF combiner whose output port is terminated
 52 in a power detector. The low frequency signal from the power detector, described by equation (14) is
 reported in Figure 6, the same signal extracted using the Matlab model is reported in Figure 7 with an

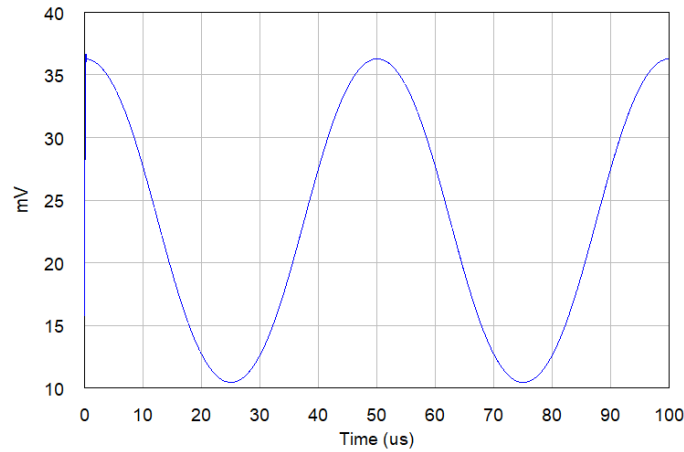


Figure 6. Low frequency signal from power detector (VSS model) with $K_p = 0.1$

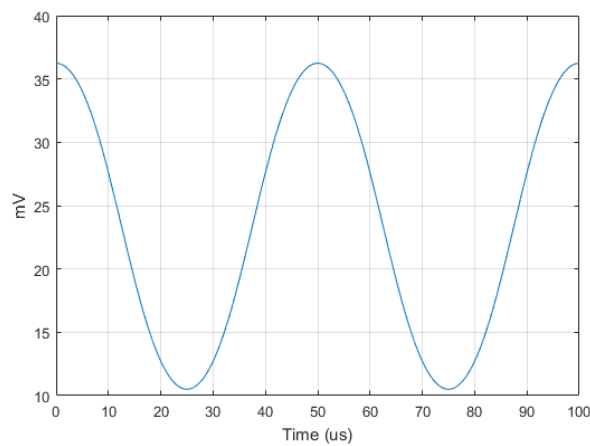


Figure 7. Low frequency signal from power detector (Matlab)with $K_p = 0.1$

53 excellent agreement between both models. The induced phase modulating signal and the recovered
 54 signal are depicted in Figure 8
 55

56 2.2. Extension to weak time-dependent amplitude modulation case

If the induced amplitude modulation is time-dependent, a signal processing approach can be adopted in order to extract the induced phase modulation. If $m_F(t)^2 \neq 1$ a more precise technique can be exploited, deleting the DC terms in (9) in post-processing. In fact, looking at Figure 9, if a generic low pass signal: $x(t) = m(t) \cos[\psi_F(t)]$ is injected in a hard limiter, the corresponding output signal can be put in the form:

$$y(t) = \text{sign}[m(t) \cos(\psi_F(t))] = \begin{cases} +1 & \text{for } |\psi_F(t)| < \frac{\pi}{2} \\ -1 & \text{for } \frac{\pi}{2} < |\psi_F(t)| < \pi \end{cases} \quad (15)$$

$$\text{with } \text{sign}(x) = \begin{cases} +1 & \text{if } x > 0 \\ -1 & \text{if } x < 0 \end{cases}$$

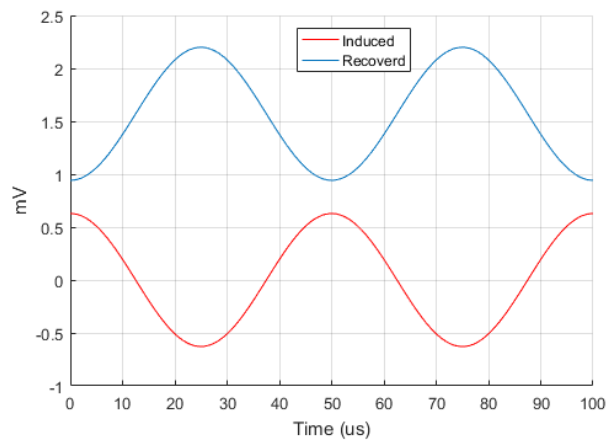


Figure 8. Induced phase noise modulating signal and recovered with $K_p = 0.1$

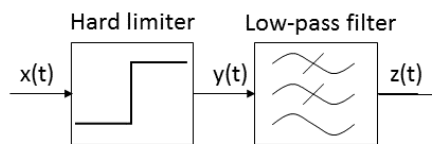


Figure 9. Signal processing approach for induced phase modulation extraction

The function $y(t)$ is periodic in ψ_F , so the corresponding Fourier series expansion can be written as:

$$y(\psi) = \sum_{n=1,3,5,\dots}^{+\infty} Y_n \cos(n\psi) \quad (16)$$

with coefficients:

$$Y_n = \frac{4 \sin\left(\frac{n\pi}{2}\right)}{n\pi} \quad (17)$$

a low-pass filter eliminates the high order harmonics so that

$$z(t) = \frac{4}{\pi} \cos[\psi_F(t)] \quad (18)$$

57 this allows to easily extract the phase induced modulation function.

58 3. High induced amplitude modulation case

When the induced amplitude modulation function $m_F(t)$ is not negligible, it is necessary to modify the test-bed in order to be able to extract the phase and the amplitude modulating functions. To this purpose, the output RF combiner is replaced by a 180° hybrid where two different power detectors are connected to the Σ and Δ ports. The output signals arising from the power detectors, eventually conveniently amplified by low noise stage amplifiers, are injected in a simultaneous sampling DaQ (Data Acquisition device). Looking at Figure 10, if the RF source generates a signal of the form (1), the signals arising from the power detectors are:

$$v_1(t) = k_{d1} A_0^2 \left(S_{32}^2 S_{2A}^2 + m_F^2(t) S_{31}^2 S_{1A}^2 + 2m_F(t) S_{31} S_{32} S_{2A} S_{1A} \cos[\phi_{up} - \phi_{down}] \right) \quad (19)$$

$$v_2(t) = k_{d2} A_0^2 \left(S_{42}^2 S_{2A}^2 + m_F^2(t) S_{41}^2 S_{1A}^2 - 2m_F(t) S_{41} S_{42} S_{2A} S_{1A} \cos[\phi_{up} - \phi_{down}] \right) \quad (20)$$

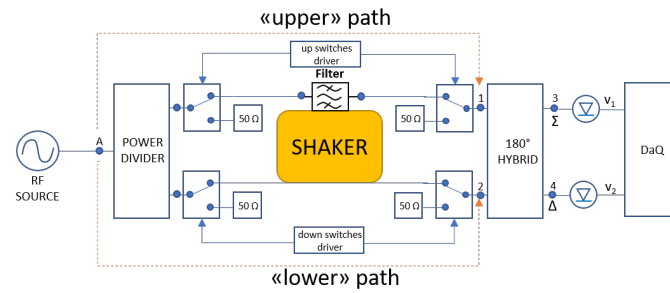


Figure 10. Extended characterisation set-up

where $S_{32}, S_{31}, S_{41}, S_{42}$ are the modules of the transmittances of the 180° hybrid and S_{1A}, S_{2A} are the modules of the transmittances of the *upper* path from node A to node 1 and *lower* path from node A to node 2 respectively. In general, the detectors sensitivity coefficients k_{d1} and k_{d2} , the parameters $S_{32}, S_{31}, S_{42}, S_{41}$ are different, even slightly, from each other. Opening the *upper* path in static conditions (no vibrations), the output voltages from the detectors are constants, respectively equal to:

$$v_1 = k_{d1} A_o^2 (S_{32}^2 S_{2A}^2) = A \quad (21)$$

$$v_2 = k_{d2} A_o^2 (S_{42}^2 S_{2A}^2) = B \quad (22)$$

closing the *upper* path, while opening the *lower*, the output voltages from the detectors are constants and respectively equal to:

$$v_1 = k_{d1} A_o^2 (S_{31}^2 S_{1A}^2) = C \quad (23)$$

$$v_2 = k_{d2} A_o^2 (S_{41}^2 S_{1A}^2) = D \quad (24)$$

Variables A, B, C, D have been introduced only to simplify the expressions in *static conditions* and allow compact notations. When vibrations are present, and both *upper* and *lower* paths are closed, the signals from the detectors are time dependent and respectively equal to:

$$v_1(t) = A + m_F^2(t)C + 2m_F(t)\sqrt{AC} \cos[\phi_{up} - \phi_d] \quad (25)$$

$$v_2(t) = B + m_F^2(t)D - 2m_F(t)\sqrt{BD} \cos[\phi_{up} - \phi_d] \quad (26)$$

after some algebraic manipulations, it is possible to write:

$$m_F(t) = \left[\frac{1}{\sqrt{\frac{C}{A}} + \sqrt{\frac{D}{B}}} \left(\sqrt{\frac{C}{A}} \frac{v_1(t) - A}{C} + \sqrt{\frac{D}{B}} \frac{v_2(t) - B}{D} \right) \right]^{\frac{1}{2}} \quad (27)$$

while the phase induced modulation is:

$$\phi_{up} - \phi_d = \psi_F(t) + \phi_{upo} - \phi_d = \cos^{-1} \left[\frac{\frac{v_1(t) - A}{C} - \frac{v_2(t) - B}{D}}{2m_F(t) \left(\sqrt{\frac{A}{C}} + \sqrt{\frac{B}{D}} \right)} \right] \quad (28)$$

59 where $\phi_{upo} - \phi_d$ are constant and vibration independent phase terms.

60 3.1. System Simulation and Validation

61 This characterisation method, as the simpler described before, has been validated through RF
 62 system simulations. The NI AWR VSS schematic is reported in Figure 11 and includes, in a more
 detailed form, the characterisation set-up depicted in Figure 10. The first part of the scheme is similar

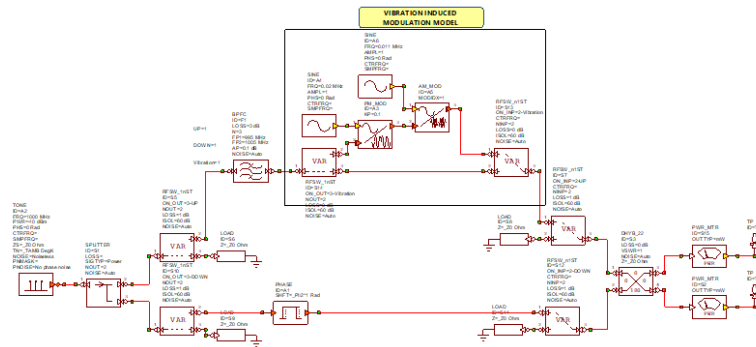


Figure 11. Extended characterisation set-up

63 to that reported in Figure 5 with two main differences: after the RF filter there are two separated
 64 amplitude and phase modulators, each of these modulates the RF signal independently from the other
 65 with different modulation frequencies and modulation indices. The signal travelling the upper path
 66 and that travelling the lower path recombines into a 180° hybrid coupler. The Σ and Δ output signals
 67 are then injected in two RF power detectors whose output voltages have been stored and processed.
 68 The vibration induced phase modulating signal is a 20 KHz unit amplitude sine wave injected in
 69 a phase modulator with a phase sensitivity coefficient $K_p = 0.1$. The vibration induced amplitude
 70 modulating signal is a 11 KHz unit amplitude sine wave injected in a amplitude modulator with a
 71 normalized sensitivity coefficient $K_m = 0.1$. The amplitude and phase modulating frequencies are not
 72 harmonically related and have been chosen different in order to verify the correct recover of both.
 73 The output voltages from the power detectors v_1 and v_2 under vibrations are reported in Figure 12

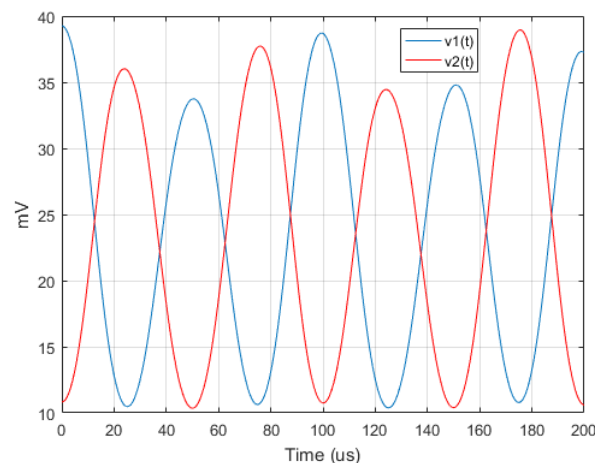


Figure 12. Low frequency signals from power detectors with $K_m = K_p = 0.1$

75 while the induced amplitude modulating signal and the one recovered are reported in Figure 13. The induced phase modulating signal and the one recovered are reported in Figure 14. For a fixed

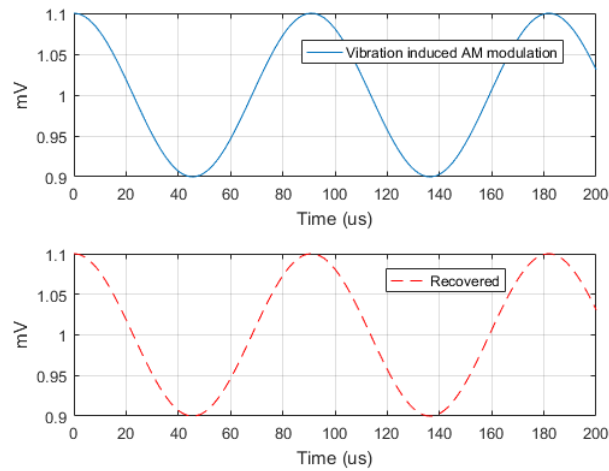


Figure 13. Vibration induced amplitude modulating signals with $K_m = K_p = 0.1$

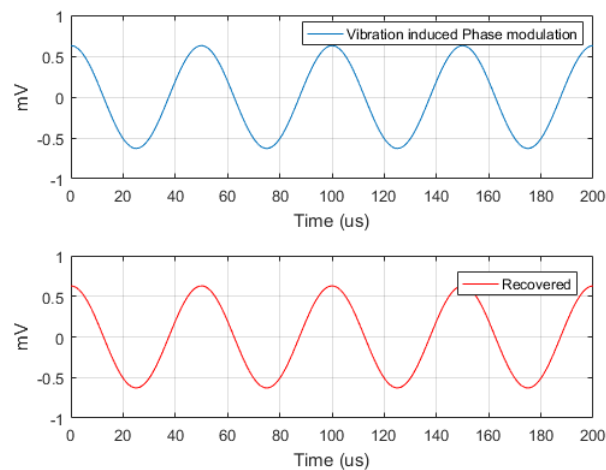


Figure 14. Vibration induced phase modulating signals with $K_m = K_p = 0.1$

76
 77 vibrational frequency, a change of the vibrational energy is modeled as a corresponding change of
 78 phase and amplitude modulation indices. If the amplitude and phase modulation indices are raised
 79 to $K_m = 0.5$ and $K_p = 0.2$ respectively, the output voltages from the power detectors v_1 and v_2
 80 are reported in Figure 15. The induced amplitude and phase waveforms and the recovered signals are
 81 reported in Figure 16 and Figure 17. It is noteworthy that the quantities: A, B, C, D can be frequency
 82 dependent, but all of them can be characterized in the frequency domain, if necessary. The quantities
 83 C, D are also allowed to be temperature-dependent as these are directly related to the transmittance
 84 of the filter under test. Moreover, the proposed method does not require a sinusoidal vibrational
 85 spectrum in order to extract the amplitude and phase induced modulations, but it can be theoretically
 86 arbitrary.

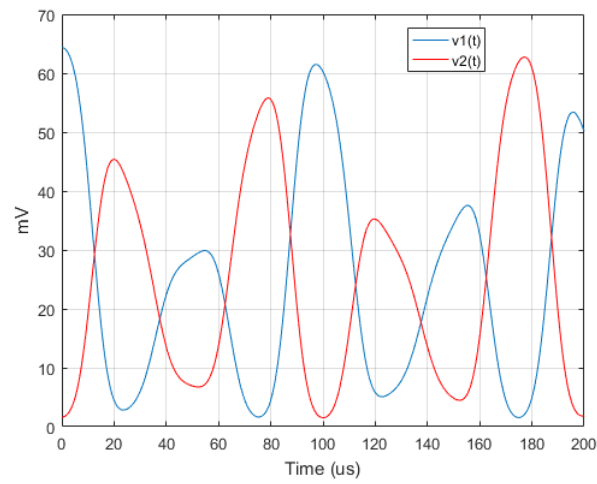


Figure 15. Low frequency signals from power detectors with $K_m = 0.5$ and $K_p = 0.2$

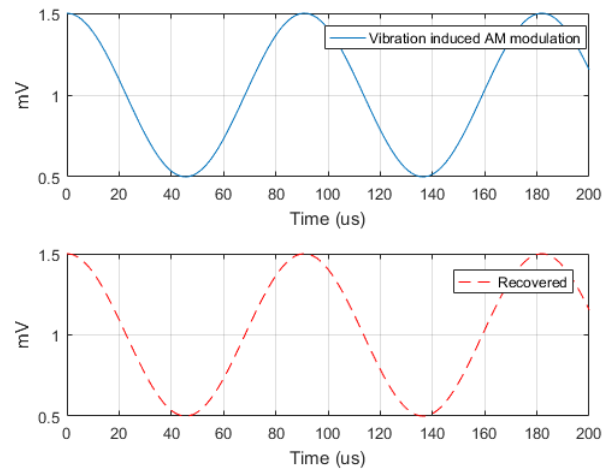


Figure 16. Vibration induced amplitude modulating signals $K_m = 0.5$ and $K_p = 0.2$

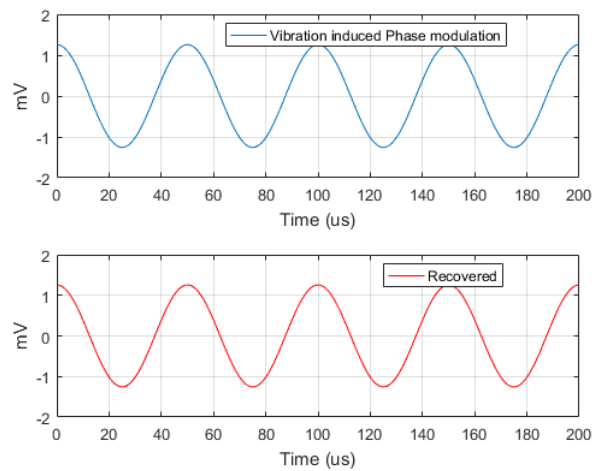


Figure 17. Vibration induced phase modulating signals $K_m = 0.5$ and $K_p = 0.2$

87 4. System Sensitivity Considerations

All the schemes discussed in previous sections works at high Signal to Noise Ratios by design, insertion losses of the devices are quite small even that of SAW filters (usually ≤ 10 [dB]). The input signal is provided by a RF source with a very high SNR while power detectors operate with signal levels ≈ 40 [dB] higher their typical tangential sensitivity [12]. Limiting the analysis to the induced phase modulation recovering, it is possible to focus the attention to equation (14) reported below for convenience, in order to derive some considerations.

$$v_1(t) = 2A_o^2 k_d S_{3Au} S_{3Ad} \cos(\psi_F(t) + \phi_0) + A_o^2 k_d S_{3Ad}^2 + A_o^2 k_d S_{3Au}^2 \quad (29)$$

If the term $\phi_0 = -\frac{\pi}{2}$, than it is possible to write

$$v_1(t) = 2k_d A_o^2 S_{3Au} S_{3Ad} \sin(\psi_F(t)) + A_o^2 k_d S_{3Ad}^2 + A_o^2 k_d S_{3Au}^2 \quad (30)$$

the induced phase modulation $\psi_F(t)$ can be assumed to be $\psi_F(t) = 2\pi K_p \cos(2\pi f_m t)$, being f_m the vibration frequency. As vibrational induced phase modulation comes from low frequency mechanical excitation (sometimes up to acoustic frequencies), it is reasonable to suppose [13] that the bandwidth BW of the signal (29) is limited to $BW \approx 2(2\pi K_p + 1) f_m < 100$ [KHz]. The estimated SNR at the output port of the RF combiner (or the output ports of the 180° hybrid) is reported in Figure 18. It can be assumed that the low frequency signal, acquired by the DaQ, is mainly contaminated by thermal noise coming from the RF section and by the intrinsic thermal noise of the device. The noise power from RF stages is $P_{nRF} \approx -124$ dBm corresponding to a RMS noise voltage $V_{nRF} \approx 0.28 \mu V$. The RMS noise voltage of a DaQ is typically much higher. For example, the National Instruments 6356 [14] in the smallest input voltage range, is characterized by a RMS noise voltage $V_n \approx 61 \mu V$, so it is prevalent over the contribution due the RF section. Small values of K_p push the system to the limit of sensibility

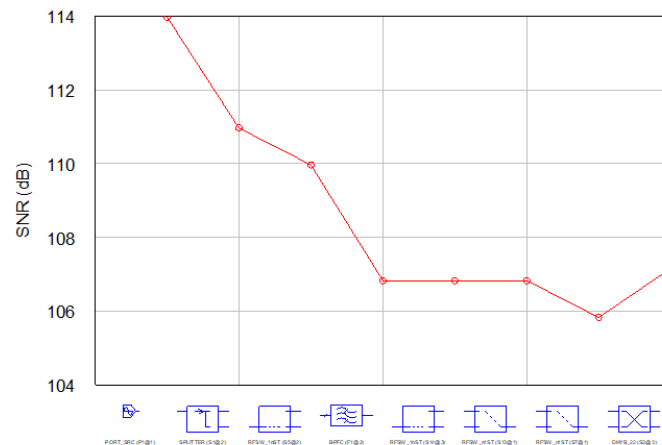


Figure 18. SNR at the output ports of the 180° hybrid

as $v_1(t)$ tends to a DC value, but at the same time, makes the filter able to operate in a severe environment. If K_p is small, it is possible to approximate the sine function in equation (30)

$$v_1(t) \approx 4k_d A_o^2 S_{3Au} S_{3Ad} \pi K_p \cos(2\pi f_m t) + A_o^2 k_d S_{3Ad}^2 + A_o^2 k_d S_{3Au}^2 \quad (31)$$

the signals measured experimentally can be written as:

$$v_1(t)^* = 4k_d A_o^2 S_{3Au} S_{3Ad} \pi K_p \cos(2\pi f_m t) + A_o^2 k_d S_{3Ad}^2 + A_o^2 k_d S_{3Au}^2 + n_o \quad (32)$$

$$v_{1_up_o_static}^* = A_o^2 k_d S_{3Ad}^2 + n_1 \quad (33)$$

$$v_{1_down_o_static}^* = A_o^2 k_d S_{3Au}^2 + n_2 \quad (34)$$

where n_o, n_1, n_2 are independent zero-mean gaussian noise components having the same standard deviation $\sigma = V_n$. As we searching for the minimum detectable phase modulation index K_p , the problem is reduced to the estimation of the amplitude of the induced modulating tone at the vibrational frequency f_m . In fact, it is possible to write

$$\frac{1}{4\pi} \frac{v_1(t)^* - v_{1_up_o_static}^* - v_{1_down_o_static}^*}{\sqrt{v_{1_up_o_static}^* v_{1_down_o_static}^*}} = K_p \cos(2\pi f_m t) + n \quad (35)$$

88 being n a gaussian noise contribution with power $P_n = \sigma^2$. In this case, a powerful tool is represented
 89 by the FFT (Fast Fourier Transform). If the DaQ operates at a sample frequency of f_s [Hz] and N
 90 samples are acquired for each signal, the FFT of the signal reported in equation (35) generates $\frac{N}{2}$
 91 points in the frequency domain where every frequency "bin" is $\frac{f_s}{M}$ [Hz] wide. A Matlab simulation has
 92 been used to estimate the parameter K_p with a relative error $\epsilon \leq 1\%$ in order to define the minimum
 93 detectable phase sensitivity coefficient K_{p_min} . The vibrational frequency has been set $f_m = 10$ [KHz]
 94 with a DaQ sample frequency $f_s = 1$ [MHz]. The effective system $SNR_{dB} = 10 \log \left(\frac{K_p^2}{2\sigma^2} \right) - G_p$ where
 95 $\frac{K_p^2}{2}$ is the signal power and $G_p = 10 \log \left(\frac{N}{2} \right)$ the processing gain of the FFT. The magnitude of the
 96 spectrum at the frequency "bin" corresponding to the vibrational frequency has been calculated while
 97 sweeping the parameter K_p , thus changing the SNR of the system and determining the relative error;
 98 the procedure has been iterated in order to obtain a distribution of the error. Some amplitude spectra
 99 are reported in Figure 19 for different values of K_p while in Figure 20 is reported the histogram fit of
 100 the relative error distribution (nearly gaussian) corresponding to the identified minimum detectable
 K_p .

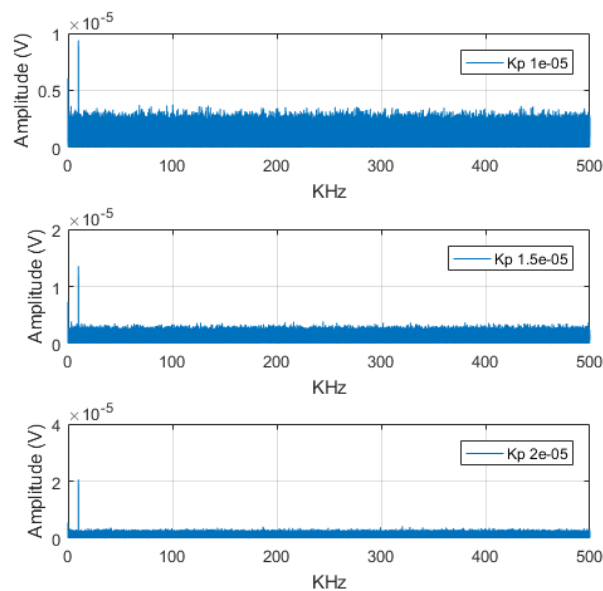


Figure 19. Amplitude spectra of signal (35) for different values of K_p

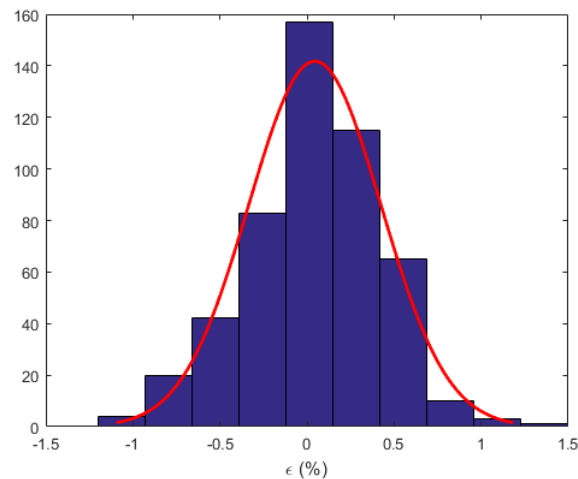


Figure 20. Histogram fit of the relative error distribution

102 From simulations it has been found a minimum detectable phase sensitivity coefficient $K_{p_{min}} \approx$
 103 $2 \cdot 10^{-4}$ [rad/V] with relative errors $\epsilon \leq 1\%$ within $3\sigma_{K_p}$.

104 5. Conclusion

105 In this paper it has been derived low-cost characterisation techniques for discrete filters under
 106 vibrations. The methods allows the extraction of both the vibration induced amplitude and phase
 107 modulation using scalar measurements only. The first technique requires few components, but is
 108 suitable for filters that exhibit negligible amplitude induced modulation. The second, more powerful
 109 and general, requires two independent power detectors that do not have to be matched. It is noteworthy
 110 to note that the proposed characterization methodology is theoretically inherently robust against the
 111 RF generator phase noise. The signals extracted by the RF power detectors depends on the *difference*
 112 between the phases of the upper and the lower paths thus erasing spurious contribution coming
 113 before the first power divider. The proposed approaches allow to characterize a microwave filter
 114 under vibrations, but also to derive behavioural models that can be used to simulate a RF chain where
 115 vibrational induced phenomena are taken into account.

116 **Conflicts of Interest:** The author declare no conflict of interest

117 References

- 118 1. MIL-STD-810G: "Environmental Engineering Considerations and Laboratory Tests", *Department Of Defence Test*
 119 *Method Standard*, 2014
- 120 2. R. L. Filler, "The acceleration sensitivity of quartz crystal oscillators: a review," in *IEEE Transactions on*
 121 *Ultrasonics, Ferroelectrics, and Frequency Control*, vol. 35, no. 3, pp. 297-305, May 1988. doi: 10.1109/58.20450
- 122 3. Hati, A.; Nelson C.W.; Howe D.A.: 'Vibration-Induced PM and AM Noise in Microwave Components', *IEEE*
 123 *Transactions on Ultrasonics, Ferroelectrics, and Frequency Control*, 2009, Volume: 56, pp.2050-2059
- 124 4. A. Hati; C. W. Nelson; D. A. Howe; N. Ashby; J. Taylor; K. M. Hudek; C. Hay; D. Seidel; D. Eliyahu : 'Vibration
 125 Sensitivity of Microwave Components', *2007 IEEE International Frequency Control Symposium Joint with the 21st*
 126 *European Frequency and Time Forum*, 2007, pp.541-546
- 127 5. Locke, S.; Sinha B.K.: 'Acceleration and Vibration Sensitivity of SAW Devices', *IEEE Transactions on Ultrasonics,*
 128 *Ferroelectrics, and Frequency Control*, 1987, Volume: 34, pp. 29-38
- 129 6. IEC 60068-2-6:2007: "Environmental testing – Part 2-6: Tests – Test Fc: Vibration (sinusoidal)", Edition 7.0 date:
 130 2007-12
- 131 7. IEC-60068-2-27:2008: "Environmental testing – Part 2-27: Tests –Test Ea and guidance: Shock", Edition 4.0 date
 132 2008-02

- 133 8. MIL-STD 801G: "Test method standard, Environmental engineering considerations and laboratory tests", 2008
- 134 9. Scott L. Miller, Donald G. Childers: "Probability and Random Processes: With Applications to Signal Processing
- 135 and Communications", Academic Press, 2012, 2012
- 136 10. National Instruments AWR VSS, [http://www.awrcorp.com/products/ni-awr-design-environment/visual-](http://www.awrcorp.com/products/ni-awr-design-environment/visual-system-simulator)
- 137 [system-simulator](http://www.awrcorp.com/products/ni-awr-design-environment/visual-system-simulator)
- 138 11. Matlab, <https://www.mathworks.com/products/matlab.html>
- 139 12. Rao, R. S.: "Microwave engineering", PHI Learning Pvt. Ltd., 2015
- 140 13. Rao, R. S.: "Communication Systems", Tata McGraw-Hill Education, 2013
- 141 14. National Instruments 6356 DaQ, [http://www.ni.com/nisearch/app/main/p/ap/tech/lang/en/pg/1/sn/](http://www.ni.com/nisearch/app/main/p/ap/tech/lang/en/pg/1/sn/ssnav:spc/aq/pmdmid:124938/)
- 142 [ssnav:spc/aq/pmdmid:124938/](http://www.ni.com/nisearch/app/main/p/ap/tech/lang/en/pg/1/sn/ssnav:spc/aq/pmdmid:124938/)